Preprint Title	Nanostructure-based electrochemical sensor: glyphosate detection and the analysis of genetic changes in rye DNA
Authors	Vjaceslavs Gerbreders, Marina Krasovska, Irena Mihailova, Andrejs Ogurcovs, Eriks Sledevskis, Andrejs Gerbreders, Edmunds Tamanis, Inese Kokina and Ilona Plaksenkova
Publication Date	16 Dez 2019
Article Type	Full Research Paper
ORCID® iDs	Marina Krasovska - https://orcid.org/0000-0002-5959-0442; Edmunds Tamanis - https://orcid.org/0000-0001-6569-4814

Nanostructure-based electrochemical sensor: glyphosate detection and the analysis of genetic changes in rye DNA

Vjaceslavs Gerbreders[1], Marina Krasovska[*1], Irena Mihailova[1], Andrejs Ogurcovs[1], Eriks Sledevskis[1], Andrejs Gerbreders[1], Edmunds Tamanis[1], Inese Kokina[2], Ilona Plaksenkova[2]

Adress: [1] G. Liberts' Innovative Microscopy Centre, Department of Technology, Institute of Life Sciences and Technology, Daugavpils University, Parades Street 1, Daugavpils LV-5401, Latvia

[2] Laboratory of Genomics and Biotechnology, Department of Biotechnology, Institute of Life Sciences and Technology, Daugavpils University, Parades Street 1A, Daugavpils, LV 5401, Latvia

Email: Marina Krasovska – marina.krasovska@du.lv

* Corresponding author

Abstract

Glyphosate, commonly known by its original trade name Roundup™, is the world's most widely used herbicide. Glyphosate and it metabolites have profound negative environmental impact and long-term toxicity risk including cancerogenity, genotoxicity, endocrine disruption even at concentration levels too low to have a herbicidal effect.

Therefore, the detection of these pollutants in low concentrations is an actual and important task.

To increase the sensitivity of the sensor, nanostructures were used.

To analyze the presence of glyphosate and its metabolites in rye juice, two groups of samples were selected. In the first case, glyphosate at different concentrations was added to the water for irrigation on the first day and then the samples were watered with pure water for 7 days. In the second case, rye was watered with pure water for all 8 days, and glyphosate was artificially added just before the measurement. The obtained samples were studied by the DPV employing nanostructured working electrode. To analyze changes in the DNA sequence, a PCR product obtained from samples of the first group was electrochemically studied. To confirm the results obtained, an electrophoresis method was also applied. The results indicate that the DPV signal obtained from samples with artificially added glyphosate has significant differences compared to the signal obtained from the juice of plants absorbing glyphosate in a natural way during growth. However, in both cases, CuO nanostructure based sensor detects the presence of glyphosate or its metabolites compared with the control sample. The experiment also found significant changes in the DNA caused by exposure with glyphosate during rye growth process of rye sprouts.

Keywords

Glyphosate detection, DNA electrochemical biosensor, CuO nanostructures, ZnO nanostructures, DPV, genetic changes.

Introduction

Glyphosate (*N*-(phosphonomethyl)glycine), widely well known as Roundup^{TM} is the most used herbicide in many countries. [1-4]. The recent researches prove undeniable negative impact of glyphosate to the environment. Even in low dosage it influences to the range of microorganisms, planktons, seaweeds, earthworms and insects, as well on health of plants (growth oppression, genetic changes, immunity deterioration and, as result, susceptibility to various fungal diseases) [5-8]. Contamination of soil and groundwater by the agent leads to environmental imbalance [9-11]. For example, a diminution in numbers of certain species of bacteria causes uncontrolled reproduction of other microorganisms, often pathogenic [12].

After treating the plants with glyphosate, it is absorbed by the plants, into the soil and water. With the degradation of about 70 % of glyphosate, a shorter molecule is formed - aminomethylphosphonic acid (aminomethylphosphonic acid or AMPA), which also has a herbicidal effect, and its toxic effect on humans is several times stronger than glyphosate itself. The content of glyphosate and AMPA in already collected soybeans is from 0.18 to 7.2 mg kg^{-1} [13].

Despite of the previously indicated low acute toxic index of glyphosate for human [14-16], the recent researches mention a long-term intoxication risk [17-20]. Even in very low concentration (less then needs for herbicide effect) the agent can cause carcinogenic [4, 6] and genotoxic effect [22] as well leads to endocrine disorders [22] and influents to fertility [23].

In the United States, a fairly high maximum glyphosate level in drinking water is allowed - 700 μg L^{-1}, in Australia even higher - 1000 μg L^{-1}, while in Europe the permissible level of pollutant is less than 0.1 μg L^{-1} [13].

Manufacturers of glyphosate-based herbicides have long convinced the public that the toxicity of such herbicides to humans is very low due to the fact that humans and other mammals lack the EPSP synthase enzyme, which is directed to the action of glyphosate in plants. However, studies of recent years do not confirm this point of view. It turned out that the study of glyphosate itself (mainly on rodents) is not enough, since the final product contains additional substances - adjuvants that accelerate the absorption of glyphosate and enhance its herbicidal effect. Comparative studies of glyphosate and the final product (RoundUp) showed that in vitro experiments on human cells, glyphosate toxicity was 2 g L^{-1}, while RoundUp 400 and 450 toxicity was 0.001 g L^{-1} [24].

Footprints of glyphosate and its metabolites can be finding in food and drinks, in soil, water and dust [25-27]. It potentially shows that everyone can be exposed the agent's detrimental impact. That is the reason why the development and the implementation of simple sensor for glyphosate determination in relatively low concentration is the important and actual task.

Different types of sensors for glyphosate detection were described in the recent publications [28-31]. Electrochemical sensors are widely used [32]. To ensure selectivity the method of functionalization (modification) of surface of working electrodes with enzymes (in particular horseradish peroxidase) were applied [33, 34]. Also quite often non-enzyme sensors were used, for example, based on copper oxide surface: the reaction between glyphosate and CuO gives the unambiguous electrochemical signal and provides a selectivity of the sensors [35, 36].

One of the most popular methods to increase the sensibility is application of nanostructured surfaces [37]. Nanostructures, due to developed surface, significantly enhance working surface of the sensor and it leads to formation of larger number of adsorption bonds [38-40].

Zinc oxide and copper oxide nanostructures have been already using in different types of gas [39, 40], heavy metal ions [39, 41-43] and bio-sensors [44-48]. These types of nanostructured oxides, made by hydrothermal methods, have several advantages compared with surfaces, modified by enzymes or others bio- and organic molecules. Firstly the oxides nanostructures preparation does not require expensive materials and complicated facilities, nor special conditions for the growth process (high temperatures, high pressure or vacuum). Secondly, ZnO and CuO nanostructure have a relatively low toxicity, as well as their raw materials required for synthesis, therefore, they do not have a negative impact on the environment. Thirdly, the hydrothermal method allows obtaining the nanostructured coatings of ZnO and CuO on solid substrates with different shapes, sizes and compositions.

The main reason why ZnO and CuO widely used as the working surface in the electrochemical biosensors is the values of their isoelectric points (8.7-10.3 and 9.5 accordingly). So their positivity at neutral pH can be used for electrostatic immobilization of molecules with less value of isoelectric points like enzymes, proteins or nucleic acids. Due their crystalline properties, the nanostructures of ZnO and CuO have relatively low solubility in biological liquids or buffer solutions that also is the advantage.

In this article we described the non-enzymatic sensor platform, based on the zinc and copper oxides nanostructures, which helps to define footprints of glyphosate and its metabolites in raw (unprocessed) juice of rye. The parallel task was determination of genetic changes appeared during of the growth of the rye sprouts in the condition of exposure with the different dosage of the glyphosate in filed water.

Materials and Methods

Preparation of the nanostructures and manufacturing of the electrochemical cell

The nanostructures of CuO were obtained by hydrothermal method. Hollow metallic cylinders made from nickel were washed with distilled water and acetone in an ultrasonic bath for 10 min. For seed layer preparation, the cylinders were fixed in the holder that provided unsputtered external surface of the cylinders. CuO seed layer was applied to the uncovered internal surface of the cylinders by magnetron sputtering method in the Kurt Lesker facility at 400 W for 135 sec. For the nanostructures growth, the cylinders were fixed in an organic glass holder. The samples had been put in the sealed glass beaker containing the working solution and were placed in preheated LINN HIGH THERM chamber (T = 90 °C). The working solution contained: 50 mL distilled water, 0.5 g $Cu(NO_3)_2$ (Sigma-Aldrich, cas#10031-43-3), 0.5 g HMTA (Sigma-Aldrich, cas# 100-97-0), and 1 g of 25 % NH_3 (Sigma-Aldrich, cas#7664-41-7). The ammonia solution helps to control the morphology and to receive a more developed surface, due to reduction of the nanostructures' dimensions.

The formation of CuO nanostructures occurs according to the dissolution – secondary precipitation mechanism in two stages, when copper hydroxide is formed at the beginning of the growth process, followed by its oxidation. The growth mechanism is described in the articles [49-52].

After 1,5 h hydrothermal treatment the cylinders with CuO nanostructures were cooled to room temperature, washed with distilled water, dried and were put in a vacuum chamber, where they were stored until the experiments.

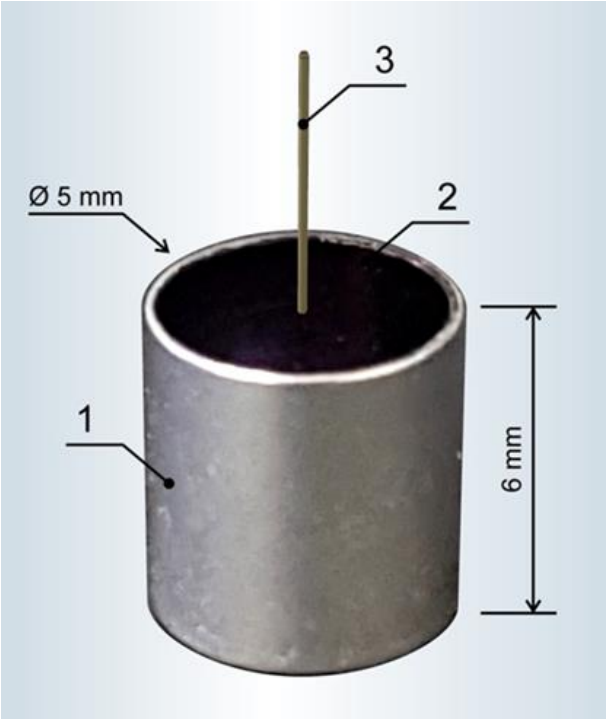

Figure 1: The electrochemical cell with CuO nanosructured layer: **1** - Ni cylinder (working electrode), **2** - CuO nanostructured layer, **3** - Pt/Ir wire (counter electrode).

For analysis of genetic changes of the rye samples, the design of the working electrodes was remade. In these experiments, the nanostructured layer of CuO was substituted with the ZnO nanotubes, previously successfully used in our laboratory for the development of a DNA sensor and heavy metal ion sensor and described in the articles [53, 54]. In addition, the cylinders were replaced to 3 mm metal discs as shown [54], that allows to reduce required volume of the analyte solution for performing the PCR products' analysis up to 3 µL.

The discs were covered by 50 mM of zinc acetate dehydrate ethanol solution and were calcinated in air at 150 °C for 30 min for ZnO seed layer receiving. As working solution 0.1 M $Zn(NO_3)_2$ (Sigma-Aldrich, cas#10196-18-6), + 0.1 M HMTA (Sigma-Aldrich, cas# 100-97-0), in distilled water was selected. The discs were immersed in the solution and were kept at 90 °C for 3 h and at 50 °C for 20 h. Detailed mechanism of the process is described in [55-59]. After that, the discs were cooled to

room temperature, were washed with distilled water, dried and were put in a vacuum chamber, where they were stored until the experiments.

The morphology of the surface of the CuO and ZnO nanostructured samples was studied by FESEM Tescan MAIA 3 facility. The chemical composition of the nanostructures has been researched by EDS Inca installation.

The crystalline structure of the samples has been defined by X-ray difractometer RIGAKU Smart Lab Cu-Kα (λ = 1.543 Å) using parallel beam scanning geometry and additional Ge(220)x2 bounce monochromator.

The electrochemical measurements have been provided by the electrochemical station Zahner. The earlier described cylinders or discs with nanostructured layers were used as working electrodes and a 0.3 mm Pt-Ir wire was used as a counter electrode (Fig. 1a).

The growth of rye sprouts under glyphosate presence and the preparation of the rye juice samples for an electrochemical analysis

For the estimation of glyphosate residues (as well as glyphosate metabolites) in the samples of rye, two types of experiments were conducted:

- Analysis of the rye juice samples that were received from the plants which had been grown in the presence of different concentrations of glyphosate solutions.
- Analysis of the pure rye juice to which glyphosate had been artificially added (in the same concentrations as in first experiment) after juice preparation.

Seeds of rye (*Secale Cereale L.* TORAF, batch PL81604335/27TD C/1) were grown in six containers on cellulose substrate. On the first day of the experiment glyphosate (Taifun B, ADAMA Agan Ltd.) was added to filed water in the following concentrations: 1 µL/50 mL, 5 µL/50 mL, 10 µL/50 mL, 50 µL/50 mL and 100 µL/50 mL. For the seven days only clear deionised water was given to the rye samples. To

the reference sample only clean water (without glyphosate) was given for all eight days. After that, the rye sprouts were grinded and pressed for juicing, which was used as an analyte without any additional treatment.

During the second type of experiments, clean water was given to all sprouts for all eight days. After the juice preparation, it was divided into 6 parts. In the five samples of the juice, the glyphosate solutions were added in the same concentrations like in the previous experiments. The sixth sample without glyphosate was used as a reference.

Both groups of samples have been studied by DPV method. The DPV measurements were conducted under following parameters: range of potential: -1000/+1200 mV, amplitude: 50 mV, step of potential: 3 mV, interval time 50 msec, modulation time: 25 msec.

Preparation of the rye sprout samples which were impacted by others stress factors during their growth process

For an estimation of other factors (not connected with glyphosate presence), the studied sprouts of rye also were growing for 8 days. The reference sample was situated in normal condition and was pouring by clear deionised water.

The glyphosate containing water (with glyphosate concentration 100 µL/50 mL) was given to the second sample only on the first day of the experiment, after that the sample was pouring by clean water.

The mineral fertilizer was added to the filed water for the third sample on the first day of the experiment, after that the sample was pouring by clean water.

The forth sample was “overdried”, it poured by clean water, but two times less often than others.

And the last one was poured every day with clean water, but it had been situated in the dark place: sprouts were grown in the condition of lack of light.

After that, the rye sprouts were grinded and pressed for juicing, which was used as an analyte without any additional treatment. The DPV measurements were conducted by the parameters described in the previous chapter.

The preparation and study of the PCR products for the estimation of genetic changes that happen after impact of glyphosate to the rye sprouts

The random amplified polymorphic DNA (RAPD) technique, as PCR-based technique, has been shown to successfully detect genotoxicity on DNA in plants [60-62]. RAPD profiling is succesfully used for evaluating of genetic effects of glyphosate on plats [63, 64].

Genomic DNA was extracted from the samples (n = 60) of the fresh 8 days old rye seedlings treated with glyphosate. The extraction has been done with slight modifications using the purification of total DNA from plant tissue Mini Protocol (DNeasy Plant Mini Kit, Qiagen GmbH, Hilden, Germany). The genomic DNA was quantified using a spectrophotometer (NanoDrop 1000, Thermo Scientific, Waltham, USA) to measure absorbance at 260 nm and the purity of DNA was checked. The stock DNA was diluted to make a working solution of 50 ng μL^{-1} for further PCR analysis.

The five RAPD primers OPA-02, OPA-07, OPA-11, OPD-18, and OPN-15 were selected for the study. PCR reactions were carried out in a thermocycler Veriti 96-WellThermal Cycler, Applied Biosystems, Foster City, USA. All PCR reactions were prepared as described in [65]. The RAPD fragments were separated and the product length was detected using a QIAxcel (Qiagen GmbH, Hilden, Germany) capillary automated electrophoresis system. The amplification reaction for each primer was

repeated twice for each sample to ensure reproducibility. Only clear and reproducible bands have been considered for analysis.

For electrochemical study of the PCR product, the primer of rye SB19 in concentration 50 ng μL^{-1} was performed on a platform previously covered by ZnO nanostructures. The samples were kept in a chamber at 24 °C and humidity 80 % for 2 h to fulfil immobilization. After that, the platforms were dried in a vacuum chamber and were stood there for storage.

The analyte contained 100 ng μL^{-1} of the PCR product in a 0.9 % NaCl solution. In each experiment the volume of the solution was 3 µL. For the estimation of hybridization degree, Methylene Blue was used as a redox indicator (the concentration was 20 µmole L^{-1}, the volume – 1 µL). Before the experiment the analyte was kept for 60 sec without voltage for the hybridization process to complete and the redox indicator was added before measurement. The DPV measurements were conducting by the same parameters as showed in 2.1.

Results and Discussion

Construction of the sensor's working electrode

The CuO and ZnO nanostructures are shown in Fig. 2. We can see that the CuO layer consist from regular, mostly vertical orientated, thin 2D-plates. The ZnO coating corresponds to a vertically oriented array of hollow tubular structures with random insignificant inclusions of non-etched nanorods.

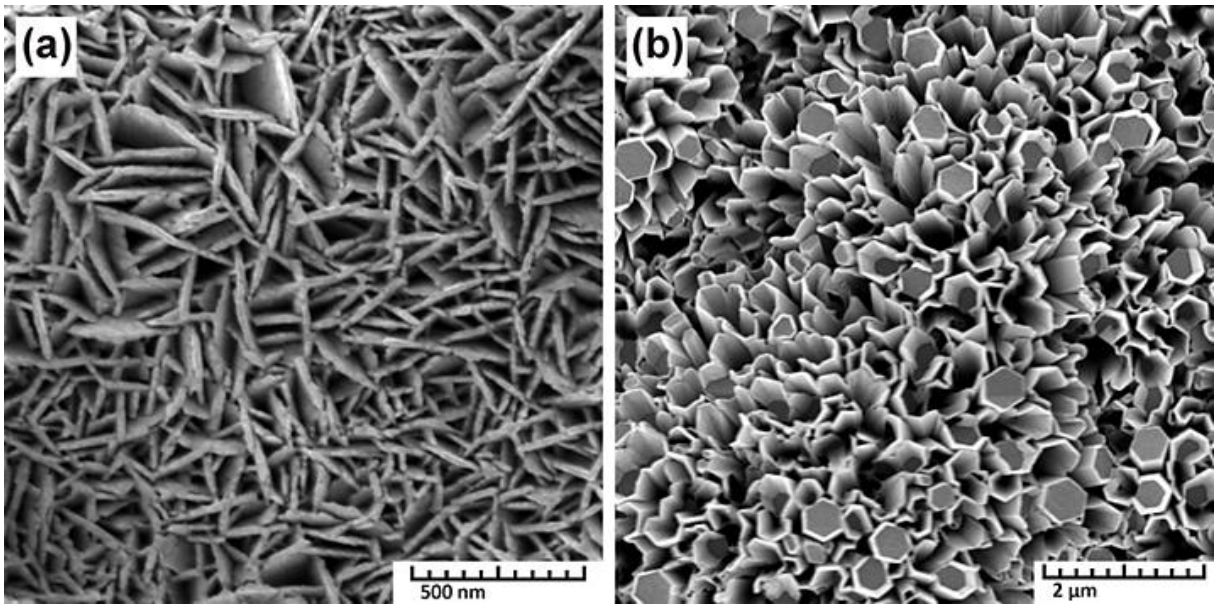

Figure 2: SEM images of CuO **(a)** and ZnO **(b)** nanostructures.

The XRD pattern (Fig. 3) shows that the both nanostructures have high degree of crystalline fracture and mostly orientated in direction of a (002) plane for ZnO and a (020) plane for CuO. Others planes are either not represented at all (in the case of CuO) or have low intensity of peaks (ZnO) that indicates alignment of the structures in a vertical z-direction.

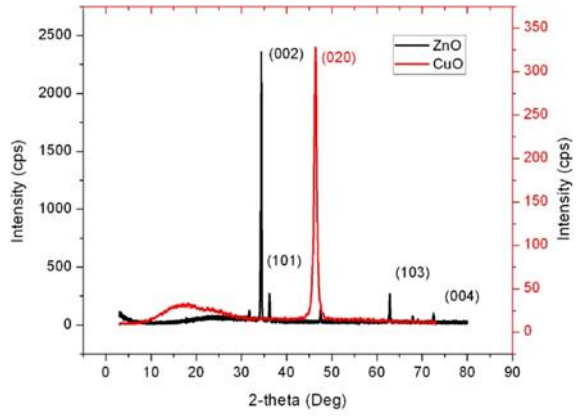

Figure 3: The results of XRD analysis for the ZnO and CuO nanolayers.

The detail descriptions of functioning of the electrochemical cells based on metal oxides nanostructures we have already published in [53].

A feature of the rye sprouts growth

Fig. 4 shows the 8-days rye sprouts. In Table 1 is presented the dependence of length of sprouts to the concentration of glyphosate that was added to the filed water. Here we can see that the average length of the sprouts reduced with augmentation of the glyphosate concentration. Even in the case of the concentration in 1000 times less then recommended by a manufacturer, the growth oppression has been observed. The degree of the oppression directly depends on the concentration of glyphosate.

Figure 4: The rye sprouts on the 8 day of the experiment. From left to right: the reference sample, the rye samples that was poured by water with the glyphosate concentrations: 1 µL/50 mL, 5 µL/50 mL, 10 µL/50 mL, 50 µL/50 mL, 100 µL/50 mL.

Table 1: The dependence of the average length of the rye sprouts on the glyphosate concentration in the filed water.

Concentration of glyphosate	Reference	1µL/50mL	5µL/50mL	10µL/50mL	50µL/50mL	100µL/50mL
Average length (cm) of sprouts	**10,88**	**9,2**	**7,78**	**7,23**	**6,45**	**5,85**

Measurements of DPV signals during the analysis of the rye sprouts juice

Electrochemical measurements show different dynamics of the dependence of the DPV peaks maximums on glyphosate concentrations for the two described experiments. In the case of the rye sprouts that were impacted by glyphosate during growth process, we can see obvious decrease of the right peak and the augmentation of the left one. In the reference sample the left peak is not observed at all, but the right one reaches of the maximum. In the cases of high concentrations of glyphosate we can see the vice versa situation: increasing of the left peak to the maximum and the disappearance of the right one.

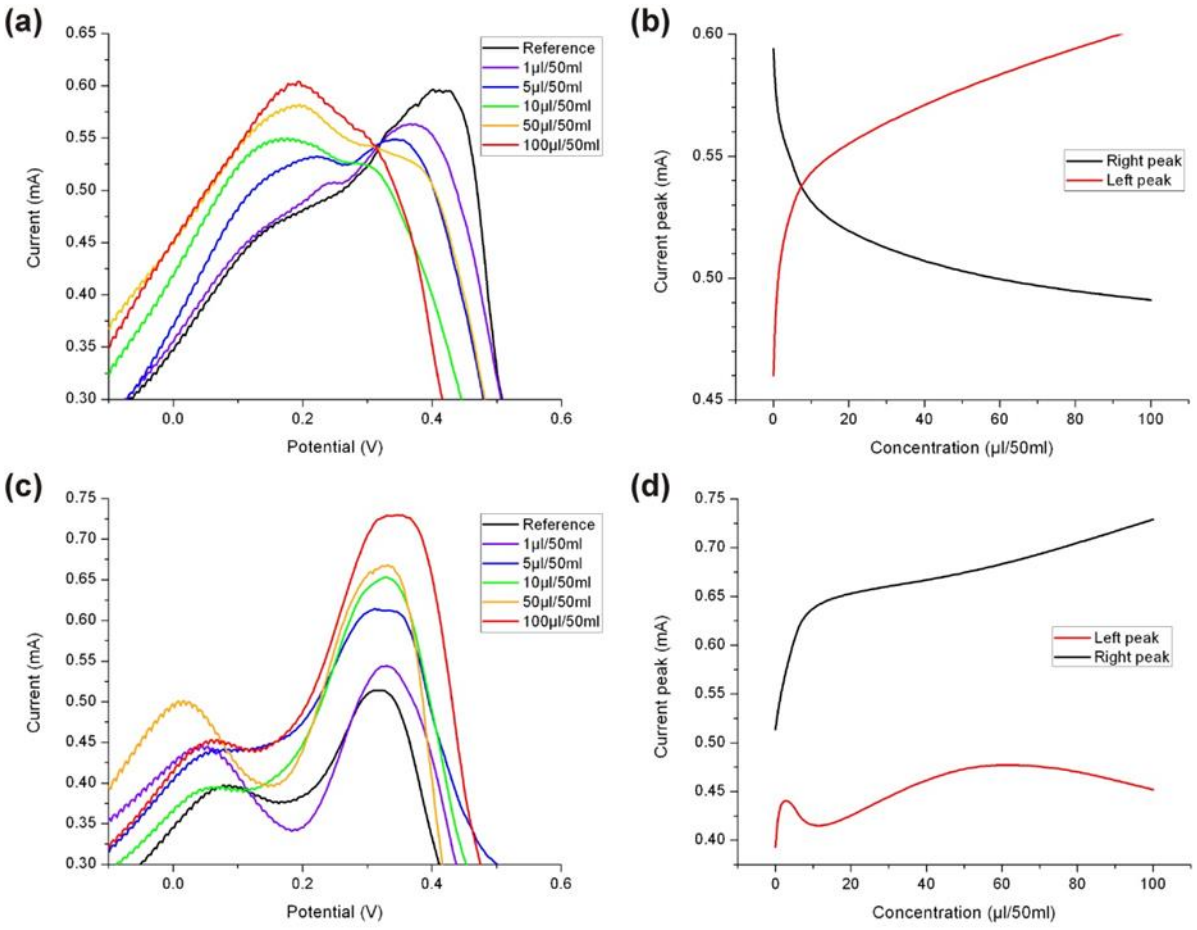

Figure 5: The DPV measurements of the rye juice samples which were impacted by the glyphosate solutions. **(a)** and **(b)**: the results have been received from the

samples which were impacted by glyphosate during of their growth. **(c)** and **(d)**: glyphosate have been added in the pure rye juice in the concentration 1 µL/50 mL, 5µL /50 mL, 10µL /50 mL, 50 µL/50 mL, 100 µL/50 mL directly before the measurements.

When glyphosate had been added in the pure juice, the augmentation of the right peak was observed that testify about common increasing of the solution conductivity. In this experiment the correlation between the left peak dynamics and the glyphosate concentration have not been observed.

This experiment proves that to obtain reliable results it is important to work with samples which have been received from sprouts and other biological materials after impacting of glyphosate during their growth rather than using the popular method of adding glyphosate artificially to pure juice, because in real conditions we are dealing with its metabolites, and not with a pure substance.

Measurements of DPV signals of the samples, which were growing under the different stress factors' impact

The results of the experiment displayed in Fig. 6.

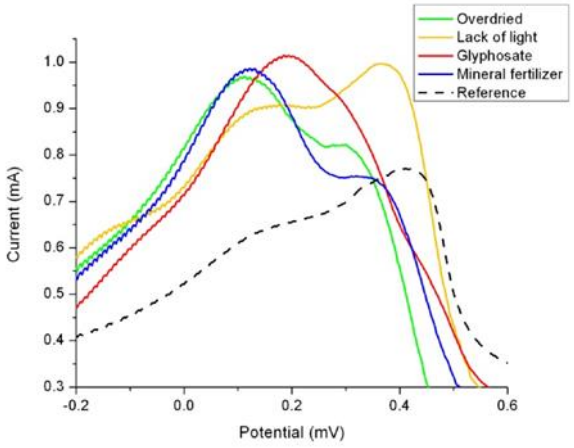

Figure 6: The curves of DPV signals that have been received from the rye sprout samples which were growing under the different impact of different stress factors.

From the experiment can make the very important conclusion: an electrochemical signal from the samples that were impacted by glyphosate during a growth process is different from the other samples which were impacted by the others stress factors. The DPV curve of the glyphosate influenced sample has the distinctive peak at approximately 0.2 V. The peak can be explain by selective interactions of glyphosate with the copper oxide nanostructures and proves the possibility of selective determination of glyphosate by this sensor.

How we can see, the curve is similar to the graph which has been received in the previous experiment for the concentration 100 µL/50 mL of glyphosate in filed water (Fig. 5a). Also, in Fig. 5a we can observe the distinctive peak at 0.2 V for the all concentrations of glyphosate.

The study of the PCR products by RAPD method

The evident changes observed in RAPD profiles such as disappearance and/or appearance of bands in comparison with the untreated control samples were evaluated and considered to be genotoxic changes. The treatment of rye plant seedlings with 1 µL/50 mL - 100 µL/50 mL glyphosate for 8 days resulted in changes in the RAPD profiles obtained from the exposed plants. RAPD profiles of plants showed disappearance of a normal band and appearance of a new band in comparison to the control. Differences in the DNA banding pattern between the reference samples and the samples treated with glyphosate were significant and were detected at different places with all utilized primers. All obtained DNA bands were polymorphic. The RAPD profiles obtained from the five oligonucleotide primers are presented in Table 2.

Table 2: *The RAPD profiles for three oligonucleotide primers.*

Primer	Reference	1µL/50mL	5µL/50mL	10µL/50mL	50µL/50mL	100µL/50mL
OPD-18	–	594	–	595	–	–
	745	743	740	–	–	–
	752	750	749	750	–	–
	758	756	755	759	–	–
	–	760	–	–	–	–
	–	1315	–	–	–	–
	–	–	–	1362	–	–
	1557	1544	–	1547	–	–
	1643	1664	–	–	–	–
	–	–	–	1729	–	–
	–	1771	–	–	–	–
	1828	–	–	–	–	–
	–	1902	–	–	–	–
	2060	–	–	–	–	–
	2099	2102	–	2103	–	–
	2117	–	–	–	–	–
	2166	–	–	–	–	–
	–	2184	–	2190	–	–
	–	–	2936	–	–	–
	–	–	2946	–	2936	2940
PB		**10**	**10**	**10**	**11**	**11**

Primer	Reference	1µL/50mL	5µL/50mL	10µL/50mL	50µL/50mL	100µL/50mL
OPA-11	786	788	–	788	–	–
	795	794	–	797	–	–
	–	–	–	1309	–	–
	2237	–	–	–	–	–
	2279	–	–	–	–	–
	–	2927	2927	–	2922	2927
PB		**3**	**5**	**3**	**5**	**5**

Primer	Reference	1µL/50mL	5µL/50mL	10µL/50mL	50µL/50mL	100µL/50mL
OPD-07	–	–	–	844	–	–
	873	–	–	870	–	–
	–	894	–	–	–	–
	1100	–	–	–	–	–
	1132	–	–	–	–	–
	1177	–	–	–	–	–
	–	–	–	–	2928	2937
	–	–	2942	–	–	–
	–	2967	–	–	2966	–
PB		**6**	**5**	**4**	**6**	**5**

According the literature, the disappearance of normal bands probably can be designated as DNA damage through modified bases, point and deletion mutations and single and double strand breaks, whereas new bands generally reveal a change in some oligonucleotide priming sites due to mutations, large deletion and/or

homologous recombination [66-68]. Overall, the RAPD results allow to conclude that all concentrations of glyphosate made significant changes in the genome of the rye plant seedlings.

Also the GTS calculations have been done by the following equitation:

$$\mathbf{GTS = (1 - a/n) \times 100}$$

where **a** is the average number of polymorphic bands, detected in treated cells and **n-**the number of total bands in the non-treated cells.

Table 3: The genomic template stability calculations result.

	Reference	**1µl/50ml**	**5µl/50ml**	**10µl/50ml**	**50µl/50ml**	**100µl/50ml**
GTS (%)	100	64,8	63,0	68,5	59,3	61,1

The experiment shows that even at the lowest concentration of glyphosate, which is more than 1000 times less then recommended by manufacturer for herbicidal effect, can lead to the genetic changes in the plant. Despite the fact that further increase of glyphosate concentration doesn't lead to significant GTS changes, the positive correlation still exist.

The minor concentration dynamics can be explained by individual features of the rye metabolism. However, the data confirms the significant genetic impact of low concentration of glyphosate to the plants.

The electrochemical studies of the PCR products

The electrochemical measurements of the PCR products on the ZnO nanostructured electrode gave the results that showed in Fig. 7.

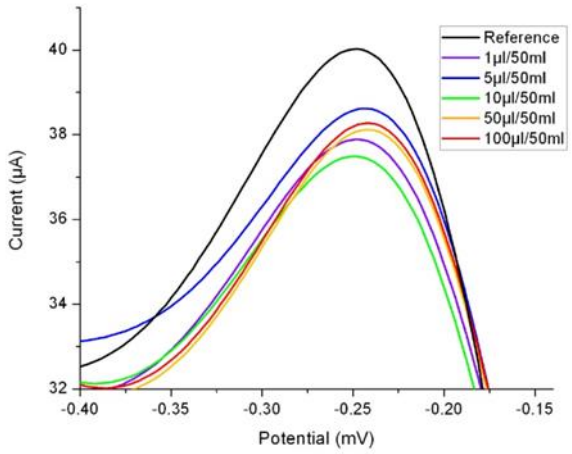

Figure 7: The curves of the DPV signals that have been received during analysis of the PCR samples of the rye sprouts which were influenced by glyphosate during their growth process.

On the graph we can see the obvious difference of the peaks maximum values between of the signal of the reference sample and the others samples. So, the method confirms appearing of genetic mutations after glyphosate influence even in small concentrations.

Probably, the peaks heights can be connected with amount of guanine fragments in the PCR products changing under glyphosate impact. As known, guanine fragments have good affinity with Methylene Blue. So, reduce of guanine amount in the DNA leads to reducing of amount of bounded MB, hence it leads to changing of the DPV signal level.

As we can see from Fig. 8, the concentration dependence of the DPV peak maximum has correlation with the GTS values for the same concentration of glyphosate. This fact confirms that the electrochemical method can be used as a precision additional method for detection of genetic changes on a par with RAPD measurements.

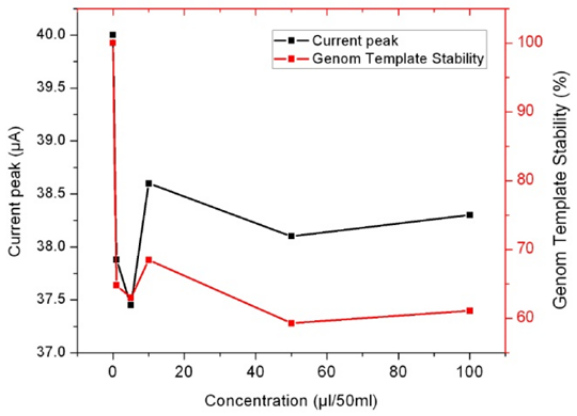

Figure 8: Comparison between the GTS values and the DPV peaks maximums for the PCR products of the rye sprouts, which were influenced by glyphosate during their growth process.

Conclusions

The presence of both pure glyphosate and its metabolites was detected in the samples of RAW juice of rye using the electrochemical sensors based on the CuO nanostructured electrodes.

Significant differences in the glyphosate concentration dependence to the electrochemical response were found for samples exposed to glyphosate during growth compared to samples to which glyphosate was added artificially. Observation data prove that the real test samples do not contain glyphosate in its pure form, but in the form of its metabolites.

The electrochemical response from the samples which have been impacted by glyphosate during the growth process of the sprouts has distinctive peak at 0.2 mV. The response is different from the curves were received after other stress factors influenced to the sprouts: addition of the mineral fertilizer, lack of water or light. The facts prove the selectivity of the sensor.

Relatively small concentrations of glyphosate (less than in 1000 times of recommended dose for herbicide effect) induce genetic changes in the rye samples. The fact was proved by RAPD method and confirmed by the electrochemical method based on the ZnO nanostructured electrode.

At glyphosate concentration increase the amount of genetic changes varies slightly but the positive dynamic was kept. It could be explained by individual features of the plant.

The electrochemical measurements results correlates with the GTS values based on the RAPD results. It proves that our electrochemical sensor based on the nanostructured electrodes can be used as the main research method and as the reference one.

Acknowledgements

This research was supported by ERDF Project No. 1.1.1.1/16/A/001 “Development of the analytical molecular recognition device based on the nanostructures of metal oxides for biomolecules detection”.

REFERENCES

1. U.S. Environmental Protection Agency. Pesticides Industry Sales and Usage 2006 and 2007 Market Estimates. In *EPA*; Grube, A.; Donaldson, D.; Kiely, T.; Wu, L., Ed.; Washington, **2011**. https://www.epa.gov/sites/production/files/2015-10/documents/market_estimates2007.pdf.
2. Székács, A.; Darvas, B. Forty Years with Glyphosate, In *Herbicides - Properties, Synthesis and Control of Weeds*; Hasaneen, M. N., Ed.; Croatia, InTech, **2012**, pp 247–284. doi:10.5772/32491

3. Krebs, C. Farmers look to broader strategies to battle weeds, *AG J.* **2011**. http://www.agjournalonline.com/features/x698043326/Farmers-look-to-broader-strategies-to-battle-weeds
4. Greim, H.; Saltmiras, D.; Mostert, V.; Strupp, C. Ch. *Crit. Rev. Toxicol.* **2015**, *45(3)*, 185–208. doi:10.3109/10408444.2014.1003423
5. Valle, L.; Mello, F. C. C.; Alves-Balvedi, R. P.; Rodrigues, L. P.; Goulart, L. R. *Environ. Chem. Lett.* **2019**, *17(1)*, 291–317. doi:10.1007/s10311-018-0789-5
6. Zhang, L.; Rana, I.; Shaffer, R. M.; Taioli, E.; Sheppard, L. *Mutat. Res.* **2019**, *781*, 186–206. doi:10.1016/j.mrrev.2019.02.001
7. Mensah, P. K.; Palmer, C. G.; Odume, O. N. Ecotoxicology of Glyphosate and Glyphosate-Based Herbicides – Toxicity to Wildlife and Humans, In *Toxicity and Hazard of Agrochemicals*; Larramendy, M. L.; Soloneski, S., Ed.; InTech, **2015**, pp 93–112. doi:10.5772/60767
8. Gill1, J. P. K.; Sethi, N.; Mohan, A.; Datta, S.; Girdhar, M. *Environ. Chem. Lett.* **2017**, *16(2)*, 401–426. doi:10.1007/s10311-017-0689-0
9. Van Bruggen, A. H. C.; He, M. M.; Shin, K.; Mai, V.; Jeong, K. C.; Finckh, M. R.; Morris, J. G. Jr. *Sci. Total Environ.* **2018**, *616-617*, 255–268. doi:10.1016/j.scitotenv.2017.10.309.
10. Gaupp-Berghausen, M.; Hofer, M.; Rewald, B.; Zaller, J. G. *Sci. Rep.* **2015**, *5*, 12886. doi:10.1038/srep12886
11. Tsui, M. T. K.; Chu, L. M. *Chemosphere* **2003**, *52(7)*, 1189–1197. doi:10.1016/S0045-6535(03)00306-0
12. Mottaa, E. V. S.; Raymanna, K.; Morana, N. A. *PNAS* **2018**, *115(41)*, 10305–10310. doi:10.1073/pnas.1803880115
13. Bai, S. H.; Ogbourne, S. M. *Environ. Sci. Pollut. Res.* **2016**, *23(19)*, 18988–19001. doi:10.1007/s11356-016-7425-3

14. Williams, G. M.; Kroes, R.; Munro, I. C. *Regul. Toxicol. Pharmacol.* **2000**, *31*, 117–165. doi:10.1006/rtph.1999.1371
15. Roberts, M.; Buckley, N. A.; Mohamed, F.; Eddleston, M.; Goldstein, D. A.; Mehrsheikh, A.; Bleeke, M. S.; Dawson, A. H. *Clin. Toxicol.* **2010**, *48(2)*, 129–136. doi:10.3109/15563650903476491
16. Beswick, E.; Millo, J. *J. Iran Chem. Soc.* **2011**, *12(1)*, 37–39. doi:10.1177/175114371101200109
17. EFSA (European Food Safety Authority), Conclusion on the peer review of the pesticide risk assessment of the active substance glyphosate, *EFSA J.*, **2015**, *13(11)*, 4302. doi:10.2903/j.efsa.2015.4302
18. Séralini, G. E.; Clair, E.; Mesnage, R.; Gress, S.; Defarge, N.; Malatesta, M.; Hennequin, D.; Spiroux de Vendômois, J. *Environ. Sci. Eur.* **2014**, *26*, 14. doi:10.1186/s12302-014-0014-5
19. Acquavella, J. F.; Alexander, B. H.; Mandel, J. S.; Gustin, C.; Baker, B.; Chapman, P.; Bleeke M. *Environ. Health Perspect.* **2003**, *112(3)*, 321–326. doi:10.1289/ehp.6667
20. Mesnage, R.; Defarge, N.; Spiroux de Vendômois, J.; Séralini, G. E. *Food Chem. Toxicol.* **2015**, *84*, 133–153. doi:10.1016/j.fct.2015.08.012
21. Bøhn, T.; Cuhra, M.; Traavik, T.; Sanden, M.; Fagan, J.; Primicerio, R. *Food Chem.* **2014**, *153*, 207–215. doi:10.1016/j.foodchem.2013.12.054
22. Pereira, G.; Jaramillo, M. L.; Remor, A. P.; Latini, A.; Davico, C. E.; da Silva, M. L.; Müller, Y. M. R.; Ammar, D.; Nazari, E. M. *Chemosphere* **2018**, *209*, 353–362. doi:10.1016/j.chemosphere.2018.06.075
23. Dallegrave, E.; Mantese, F. D.; Oliveira, R. T.; Andrade, A. J. M.; Dalsenter, P. R.; Langeloh, A. *Arch. Toxicol.* **2007**, *81(9)*, 665–673. doi:10.1007/s00204-006-0170-5

24. Gasnier, C.; Dumont, C.; Benachour, N.; Clair, E.; Chagnon, M-C.; Séralini, G. E. *Toxicol.* **2009**, *262(3)*, 184–191. doi:10.1016/j.tox.2009.06.006
25. Mesnage, R.; Bernay, B.; Séralini, G.-E. *Toxycol.* **2013**, *313(2–3)*, 122–128. doi:10.1016/j.tox.2012.09.006
26. EFSA (European Food Safety Authority), The 2011 European Union report on pesticide residues in food, *EFSA J.* **2014**, *12(5)*, 3694. doi:10.2903/j.efsa.2014.3694
27. Majewski, M. S.; Coupe, R. H.; Foreman, W. T.; Capel, P. D. *Environ. Toxicol. Chem.* **2014**, *33*, 1283–1293. doi:10.1002/etc.2550
28. Noori, J. S.; Dimaki, M.; Mortensen, J.; Svendsen, W. E. *Sensors* **2018**, *18(9)*, 2961. doi:10.3390/s18092961
29. Do, M. H.; Florea, A.; Farre, C.; Bonhomme, A.; Francois, B.; Vocanson, F.; Trang, T. T. N.; Jaffrezic-Renault, N. *Int. J. Environ. Anal. Chem.* **2015**, *95(15)*, 1489–1501. doi:10.1080/03067319.2015.1114109
30. De Almeida, L. K .S.; Chigome, S.; Torto, N.; Frost, C. L.; Pletschke, B .I. *Sens. Actuators B Chem.* **2015**, *206*, 357–363. doi:10.1016/j.snb.2014.09.039
31. González-Martínez, M. Á.; Brun, E. M.; Puchades, R.; Maquieira, Á.; Ramsey, K.; Rubio, F. *Anal. Chem.* **2005**, *77(13)*, 4219-4227. doi:10.1021/ac048431d
32. Barbosa, P. F. P.; Vieira, E. G.; Cumba, L. R.; Paim, L. L.; Nakamura, A. P. R.; Andrade, R. D. A,; Ribeiro do Carmo, D. *Int. J. Electrochem. Sci.* **2019**, *14*, 3418 – 3433. doi:10.20964/2019.04.60
33. Songa, E. A.; Arotiba, O. A.; Owino, J. H. O.; Jahed, N.; Baker, P. G. L.; Iwuoha, E. I. *Bioelectrochem.* **2009**, *75*, 117–123. doi:10.1016/j.bioelechem.2009.02.007
34. Cahuantzi-Muñoz, S. L.; González-Fuentes, M. A.; Ortiz-Frade, L. A.; Torres, E.; Ţălu, Ş.; Trejo, G.; Méndez-Albores, A. *Electroanalysis* **2019**, *31*, 1– 10. doi:10.1002/elan.201800759

35. Pooraho, S.; Thammakhet, C.; Thavarungkul, P.; Kanatharana, P. *Chem. Pap.* **2015**, *69(3)*, 385–394. doi:10.1515/chempap-2015-0038
36. Chang, Y. C.; Lin, Y. S.; Xiao, G. T.; Chiu, T. C.; Hu, C. Ch. *Talanta* **2016**, *161*, 94–98. doi:10.1016/j.talanta.2016.08.029
37. Huang, X. J.; Choi, Y. K. *Sens. Actuators B* **2007**, *122*, 659–671. doi:10.1016/j.snb.2006.06.022
38. Wang, X.; Cai, W.; Liu, S.; Wang, G.; Wua, Z.; Zhaoc, H. *Colloids and Surfaces A: Physicochem. Eng. aspects* **2013**, *422*, 199–205. doi:10.1016/j.colsurfa.2013.01.031
39. Wang, X.; Guo, Y.; Yang, L.; Han, M.; Zhao, J.; Cheng, X. *J. Environ. Anal. Toxicol.* **2012**, *2(7)*, 154. doi:10.4172/2161-0525.1000154
40. Chang , J.; Ahmad, M. Z.; Wlodarski, W.; Waclawik, E. R. *Sensors* **2013**, *13(7)*, 8445–8460. doi:10.3390/s130708445
41. Rahman, M. M.; Khan, S. B.; Marwani, H. M.; Asiri, A. M.; Alamry, K. A.; Rub, M. A.; Khan, A.; Khan, A. A. P.; Qusti, A. H. *J. Industr.Eng. Chem.* **2014**, *20*, 1071–1078. doi:10.1016/j.jiec.2013.06.044
42. Khan, S. B.; Rahman, M. M.; Marwani, H. M.; Asiri, A. M.; Alamry, K. A. *Nanoscale Res. Lett.* **2013**, *8*:377. doi:10.1186/1556-276X-8-377.
43. Kikuchi, Y.; Qian, Q.; Machida, M.; Tatsumoto, H. *Carbon* **2006**, *44(2)*, 195–202. doi:10.1016/j.carbon.2005.07.040
44. Luz, R. A. S.; Iost, R. M.; Crespilho, F. N. Nanomaterials for Biosensors and Implantable Biodevices. In *Nanobioelectrochemistry*; Crespilho, S., Ed.; Springer-Verlag Berlin Heidelberg, **2013**, pp 27–48. doi:10.1007/978-3-642-29250-7_2
45. Das, M.; Sumana, G.; Nagarajan, R.; Malhotra, B. D. *Thin Solid Films*, **2010**, *519(3)*, 1196–1201. doi:10.1016/j.tsf.2010.08.069

46. Tak, M.; Gupta, V.; Tomar, M. *Biosens. Bioelectron.* **2014**, *59*, 200–207. doi:10.1016/j.bios.2014.03.036
47. Mohammed, M.; Ibraheem, I. J.; Obaid, A. S.; Bououdina, M. *Sens. Bio-Sens. Res.*, **2017**, *15*, 46–52. doi:10.1016/j.sbsr.2017.07.003
48. Verma, R.; Sood, S.; Singh, R.; Sumana, G.; Bala, M.; Sharma, V. K.; Samantary, J. C.; Padney, R. M.; Manholta, B. D. *Diagn. Microbiol. Infect. Disease* **2014**, *78*, 16–23. doi:10.1016/j.diagmicrobio.2013.09.010
49. Hou, L.; Zhang, C.; Li, L.; Du, C.; Li, X.; Kang, X. F.; Chen, W. *Talanta* **2018**, *188*, 41–49. doi:10.1016/j.talanta.2018.05.059
50. Zhang, Q.; Zhang, K.; Xu, D.; Yang, G.; Huang, H.; Nie, F.; Liu, C.; Yang, S. *Progress Mat. Sci.*, **2014**, *60*, 208–337. doi:10.1016/j.pmatsci.2013.09.003
51. Sonia, S.; Poongodi, S.; Kumar, P. S.; Mangalaraj, D.; Ponpandian, N. *Mat. Sci. Semiconductor Proc.* **2015**, *30*, 585–591. doi:10.1016/j.mssp.2014.10.012
52. Nakate, U. T.; Lee, G. H.; Ahmad, R.; Patil, P.; Hahn, Y. B.; Yu, Y.T.; Suh, E.K. *Int. J. Hydrogen Energy* **2018**, *43*, 22705–22714. doi:10.1016/j.ijhydene.2018.09.162
53. Krasovska, M.; Gerbreders, V.; Mihailova, I.; Ogurcovs, A.; Sledevskis, E.; Gerbreders, A.; Sarajevs, P. *Beilstein J. Nanotechnol.* **2018**, *9*, 2421–2431. doi:10.3762/bjnano.9.227
54. Gerbreders, V.; Krasovska, M.; Mihailova, I.; Ogurcovs, A.; Sledevskis, E.; Gerbreders, A.; Tamanis, E.; Kokina, I.; Plaksenkova, I. *Sens. Bio-Sens. Res.* **2019**, *23*, 100226. doi:10.1016/j.sbsr.2019.100276
55. Krasovska, M.; Gerbreders, V.; Paskevics, V.; Ogurcovs, A.; Mihailova, I. *Latvian J. Phys. Technic. Sci.* **2015**, *52(5)*, 28–40. doi:10.1515/lpts-2015-0026
56. Krasovska, M.; Gerbreders, V.; Tamanis, E.; Gerbreders, S.; Bulanovs, A *Latvian J. Phys. Technic. Sci.* **2017**, *54(1)*, 41–50. doi:10.1515/lpts-2017-0005

57. Chae, K. W.; Zhang, Q.; Kim, J. S.; Jeong, Y. H., Cao, G. *Beilstein J. Nanotechnol.* **2010**, *1*, 128–134. doi:10.3762/bjnano.1.15

58. Roza, L.; Rahman, M. Y. A.; Umar, A. A.; Salleh, M. M. *J. Alloys Comp.* **2014**, *618*, 153–158. doi:10.1016/j.jallcom.2014.08.113

59. Xi, Y.; Song, J.; Xu, S.; Yang, R.; Gao, Z.; Hu, C.; Wang, Z. L. *J. Mater. Chem*. **2009**, *19*, 9260–9264. doi:10.1039/b917525c

60. Moreno-Olivas, F.; Gant Jr., V. U.; Johnson, K. L.; Peralta-Videa, J. R.; Gardea-Torresdey, J. L. *Zhejiang Univ.-Sci. A (Appl. Phys. & Eng.)* **2014**, *15(8)*, 618–623. doi:10.1631/jzus.A1400159

61. Bhaduri, M.; Fulekar, M. H. *Soil Sediment Contamin. : Int. J.* **2015**, *24(4)*, 411–422. doi:10.1080/15320383.2015.970683

62. Sorrentino, M. C.; Capozzi, F.; Giordano, S.; Spagnuolo, V. *Chemosphere* **2017**, *181*, 208–215. https://doi.org/10.1016/j.chemosphere.2017.04.065

63. Nardemir, G.; Agar, G.; Arslan, E.; Erturk, F. A. *Theor. Exp. Plant Physiol.* **2015**, *27*, 131–139. doi:10.1007/s40626-015-0039-1

64. Silprasit, K.; Ngamniyom, A.; Kerksakul, P.; Thumajitsakul, S. *App. Environ. Res.* **2016**, *38(1)*, 75–85. doi:10.35762/AER.2016.38.1.7

65. Kokina, I.; Jahundoviča, I.; Mickeviča, I.; Sledevskis, E.; Ogurcovs, A.; Polyakov, B.; Jermaļonoka, M.; Strautiņš, J.; Gerbreders, V. *J. Nanomater.* **2015**, *2015(1)*, 1–7. doi:10.1155/2015/470250

66. Pandey, C; Gupta, M. *J. Hazard. Mat.* **2015**, *287*, 384–391. doi:10.1016/j.jhazmat.2015.01.044

67. Ackova, G.; Kadifkova-Panovska, T.; Andonovska, K. B.; Stafilov, T. *J.Environ. Sci. Health B* **2016**, *51(5)*, 40–349. doi:10.1080/03601234.2015.1128747

68. Venkatachalam, P.; Jayalakshmi, N.; Geetha, N.; Sahi, S. V.; Sharma, N. C.; Rene, E. R.; Sarkar, S. K.; Favas, P. J. C. *Chemosphere* **2017**, *171*, 544–553. doi: 10.1016/j.chemosphere.2016.12.092